Relationship between Conserved Consensus Site Residues and the Productive Conformation for the TPQ Cofactor in a Copper-Containing Amine Oxidase from Yeast†

Benjamin Schwartz,‡ Edward L. Green,§ Joann Sanders-Loehr,§ and Judith P. Klinman*,‡

Departments of Chemistry and Cell and Molecular Biology, University of California, Berkeley, California 94720, and Department of Biochemistry and Molecular Biology, Oregon Graduate Institute of Science and Technology, Portland, Oregon 97291-1000

Received June 29, 1998; Revised Manuscript Received September 8, 1998

ABSTRACT: A highly conserved asparagine residue is contained in the consensus site sequences of all known copper-containing amine oxidases (CAOs). On the basis of published crystallographic structures, the asparagine is found to reside proximal to the active site redox cofactor, 2,4,5-trihydroxyphenylalanine quinone (TPQ). In this study, the conserved asparagine was changed to an alanine in a CAO from *Hansenula polymorpha* expressed in *Saccharomyces cerevisiae*, and the mutant's catalytic properties were characterized using steady-state kinetics and resonance Raman spectroscopy. Several lines of evidence point to TPQ exisiting in an nonproductive orientation in the mutant, including reductions in several steady-state parameters and an accumulation of an inactive product Schiff base complex when the enzyme is incubated with methylamine as the substrate. This product Schiff base complex was previously found to form following mutation of another conserved consensus site residue, a glutamate (or aspartate) at the C + 1 position from TPQ [Cai, D., Dove, J., Nakamura, N., Sanders-Loehr, J., and Klinman, J. P. (1997) *Biochemistry 36*, 11472−11478]. The results suggest that these two residues are crucial in maintaining the balance of cofactor mobility versus rigidity expected to be necessary during the dual processes of biogenesis and catalysis, respectively, that all CAOs must accomplish. In addition, a previously unidentified structural linkage between these two highly conserved residues is proposed which spans both subunits of the dimeric CAOs, and may have implications for intersubunit communication.

Copper-containing amine oxidases (CAOs)[1] catalyze the two-electron oxidative deamination of amines:

$$RCH_2NH_3^+ + O_2 + H_2O \rightarrow RCHO + H_2O_2 + NH_4^+$$

CAOs have been found in a wide variety of organisms, including bacteria, yeast, plants, and mammals (*1*). In prokaryotic organisms, these enzymes are utilized for growth on amines; however, in eukaryotes, the physiological role of CAOs is less well defined. Recently, the activity of one class of CAOs, also called semicarbazide-sensitive amine oxidases or SSAOs, has been found to be correlated with certain chronic medical conditions in diabetic patients, such as nephropathy. This is due to the formation of atherosclerotic plaques, likely caused by an increase in the extent of nondiscriminate protein modification by certain aldehyde products of CAO-catalyzed reactions (*2*). The formation of vascular plaques resulting from CAO activity has also been implicated as a possible factor contributing to congestive heart failure in humans (*3*).

The redox cofactor in all CAOs studied to date has been shown to be 2,4,5-trihydroxyphenylalanine quinone (TPQ or TOPA quinone), which arises from post-translational modification of a specific tyrosine residue within the protein (*4*−*6*). This process has been shown to be autocatalytic in the presence of molecular oxygen; no additional enzymes or cofactors are necessary for the transformation of protein-bound tyrosine to TPQ (*7*, *8*).

In addition to containing TPQ, all known CAOs have the consensus site sequence Asn-Tyr*-Asp/Glu-Tyr/Asn (residues 404−407 in the yeast enzyme) (*9*). Tyr405 is the residue in the nascent amine oxidase from the yeast *Hansenula polymorpha* (HPAO) that becomes modified to TPQ. Crystal structures of CAOs from various sources have recently been solved (*10*−*13*), providing a basis for the prediction of the roles of the consensus site residues in catalysis and biogenesis. However, little detailed mechanistic work has been done to date to corroborate such predictions.

In this paper, Asn404 has been mutated to an alanine, resulting in several lines of evidence which indicate that this residue is critical in the proper positioning of the TPQ cofactor during catalysis. Although the mutant enzyme is able to turn over, the TPQ ring can adopt nonproductive binding modes at several junctures along the catalytic

† This work was supported by National Institutes of Health grants to J.P.K. (GM 39296) and to J.S.-L. (GM 34468). B.S. was supported by National Institutes of Health Postdoctoral Fellowship GM 18813.

* To whom correspondence should be addressed.

‡ University of California.

§ Oregon Graduate Institute of Science and Technology.

[1] Abbreviations: TPQ or TOPA quinone, 2,4,5-trihydroxyphenylalanine quinone; WT, wild-type; PSB, product Schiff base; CAO, copper-containing amine oxidase; SSAO, semicarbazide-sensitive amine oxidase; HPAO, amine oxidase from yeast strain *Hansenula polymorpha*; BSAO, bovine serum amine oxidase; IS, ionic strength.

10.1021/bi981541s CCC: $15.00
Published on Web 11/05/1998

pathway, leading to a decline in catalytic efficiency. These results are similar to those found previously with another consensus site mutant, E406N, and may be an indication of an important spatial linkage between these residues.

MATERIALS AND METHODS

Mutagenesis, Expression, and Protein Purification of N404A in Yeast. Mutagenesis of the amine oxidase gene from *H. polymorpha* (in a pDB20 plasmid) was performed with the Chameleon double-stranded, site-directed mutagenesis kit (Strategene Cloning Systems) using *Aat*II as the selection endonuclease. The sequence of the mutagenic primer (purchased from Operon Technologies, Inc.) was 5′-ATATTTACTGCTGCC**GCT**TACGAGTACTGTCTG-3′. The mutated codon is underlined, and the mutated nucleotides are bold. The sequence of the mutated gene was established by sequencing a stretch of DNA from 30 to −30 bases from the mutated base pair(s) using a T7 Sequenase kit (UCB). Expression in *Saccharomyces cerivisae* was carried out by transforming strain CG379 using a lithium acetate procedure (*14*). Mutants were maintained on plates of URA^- media supplemented with an amino acid solution (20 mL per liter of plates) containing 5 g of adenine, histidine, and tryptophan and 7.5 g of leucine per liter.

N404A was purified like other HPAO mutants (*15*). The protein concentration was determined using a Bradford assay (Bio-Rad Laboratories); bovine serum albumin was used as the protein standard. The TPQ concentration was determined by reaction of the enzyme with phenylhydrazine (*8*).

Materials. CH_3NH_2·HCl, CD_3NH_2·HCl, $CH_3CH_2NH_2$·HCl, and $C_6H_5CH_2CH_2NH_2$·HCl were purchased from Aldrich (Milwaukee, WI). UV−vis spectroscopy was performed on a HP8452A spectrophotometer fitted with a constant-temperature bath. Rates of oxygen consumption were determined on a YSI oxygen electrode (Yellow Springs Instrument Co., Inc., Yellow Springs, OH).

Buffer Preparation. Kinetic experiments using the oxygen electrode and UV−vis spectrophotometer were carried out in 100 mM phosphate (pH range of 6−8) or pyrophosphate (pH range of 8−9) buffers adjusted to a constant ionic strength (IS = 300 mM) with potassium chloride, similar to conditions used for kinetic determinations with WT HPAO (*16*). Assays conducted in the electrode had a total volume of 1.0 mL, while those in the spectrophotometer had a total volume of 100 μL.

Steady-State Kinetic Measurements. The reactions catalyzed by WT and mutant HPAO were followed by measuring the initial rates of oxygen consumption on an oxygen electrode at 25 °C. k_{cat}/K_m values with respect to amine as the substrate were determined by measuring initial velocities while varying concentrations of amine. k_{cat}/K_m values with respect to oxygen as the substrate were determined by measuring initial rates at varying oxygen tensions, generated by pre-equilibration of assay solutions with varying mixtures of nitrogen and oxygen. k_{cat} and k_{cat}/K_m values were obtained by fitting the data directly to the Michaelis−Menten equation using the program Kaleidagraph.

Inactivation of N404A with Methylamine. Inactivation of the mutant protein was followed spectrophotometrically as follows. The purified protein was added to a quartz cuvette to a final concentration of 10 μM TPQ in buffers at various pHs and at an IS of 300 mM at 25 °C (see above). After an initial spectrum was collected, a 1−2 μL aliquot of methylamine stock solution equal to 10 times the K_m of the substrate was added, and spectra were collected at 30 s intervals during the duration of the inactivation. Inactivation was monitored by following the absorbance increase at 380 nm (*17*) and quantified by measuring the rates of absorbance change with respect to time for each reaction.

Reactivation of N404A. A 100 μL solution containing 10.0 μM mutant protein and 5 mM methylamine was allowed to react at pH 9.0 and 25 °C and the reaction followed spectrophotometrically until formation of the 380 nm peak ceased (1.5 h). The reaction mixture was dialyzed [3 × 100 μL of 10 mM pyrophosphate buffer (pH 9.0)] and finally concentrated using a Microcon microconcentrator (Amicon, Inc.). The resultant 5−10 μL aliquot of inactivated enzyme was then immediately added to a 95 μL solution of buffer, and the decay of the 380 nm peak was followed at various pHs. The decline of the peak was fit to a first-order exponential to determine the rate of reactivation.

Biogenesis of N404A from Yeast. The biogenesis of TPQ was followed qualitatively by heating the enzyme at 37 °C and taking spectra at regular intervals over the course of 24 h.

The rate of biogenesis was determined at 30, 37, and 45 °C by incubating samples of the enzyme in a constant-temperature water bath and removing aliquots at regular time intervals for cofactor quantitation by reaction with phenylhydrazine.

Resonance Raman Sample Preparation. A stock solution of N404A (0.88 mM protein monomer and 0.5 mM TPQ) was prepared in pyrophosphate buffer (IS = 200 mM, pH 9.0). Adducts were prepared by the addition of methylamine (final concentrations of 0.17 M methylamine and 0.42 mM TPQ) to a 10 μL sample of stock solution; substrate was added at >300-fold excess over protein due to the large value of k_{cat} relative to k_{inact} (ratio of 265). Isotope labeling of inactivated enzyme was performed by the addition of [$^2H_3$]-methylamine (98% D atom, Aldrich). A D_2O protein sample was prepared by diluting a portion of the stock solution into a 10-fold excess of deuterated pyrophosphate buffer (IS = 200 mM, pH 9.0) and concentrating back to 0.88 mM protein with a Microcon 30 microconcentrator (Amicon), followed by exchange for 20 h at 4 °C. Then, methylamine was added to yield final concentrations of 0.17 M amine and 0.42 mM TPQ.

Resonance Raman Spectroscopy. Raman spectra were obtained on a McPherson 2061 spectrograph (0.67 m, 2400 groove grating) using a Kaiser Optical holographic supernotch filter and a Princeton Instruments (LN-1100PB) liquid N_2-cooled CCD detector. The excitation source was a Coherent Innova 302 Kr laser. Spectra were collected from samples in capillary tubes, cooled to ice temperature in a copper coldfinger, using 413.1 nm excitation (20 mW), 90° scattering geometry, 4 cm^{-1} spectral resolution, and data accumulation for 15 min. Peak frequencies were calibrated relative to an indene standard and are accurate to ±1 cm^{-1}. Spectra of samples substituted with isotopes were obtained under identical instrumental conditions such that frequency shifts are accurate to ±0.5 cm^{-1} (*18*).

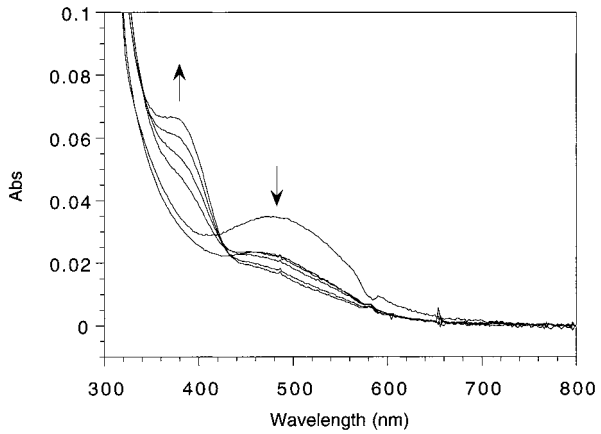

FIGURE 1: Formation of the PSB complex with methylamine. UV−vis spectra showing the time course for the formation of the adduct at pH 9. The peak at 480 nm (descending) represents oxidized TPQ, while the peak at 380 nm (ascending) represents the PSB adduct. Time points are shown at 0, 1, 10, 20, 40, and 60 min.

RESULTS

Inactivation of N404A with Methylamine. A previous mutant of HPAO (E406N) displayed rapid, reversible inhibition when incubated with methylamine (*17*). The inactivated species displayed a characteristic absorbance at 380 nm, which was shown to be due to the deprotonated product Schiff base (PSB) by resonance Raman spectroscopy. When N404A was incubated with methylamine, a similar 380 nm peak was observed to accumulate over time (Figure 1). As with E406N, this peak was not formed when N404A was incubated with larger substrates, such as ethylamine or phenethylamine.

The Raman spectrum with E406N (Figure 2A) was dominated by a C═N stretch at 1622 cm^{-1} that shifted 59 cm^{-1} to lower energy upon deuteration of the substrate methyl group (Figure 2C) and was unaffected by deuteration of the amino group (Figure 2B) (*17*). Similar deprotonated PSB species have been observed for methylamine adducts of native phenethylamine oxidase from *Arthrobacter globiformis* and bovine serum amine oxidase, where the C═N stretching assignment was further verified by a −19 cm^{-1} shift with $CH_3{}^{15}NH_2$ (*19*). The spectrum of the N404A adduct is similarly dominated by an intense feature at 1622 cm^{-1} (Figure 2D) that undergoes a similar shift of −58 cm^{-1} with CD_3NH_2 (Figure 2F), thereby identifying this peak as the C═N stretch of the PSB. As in the case of E406N, the N404A adduct failed to exhibit any shift in the C═N stretch with CH_3ND_2 in D_2O (Figure 2E), thereby indicating a lack of exchangeable protons on the C═N moiety. The D_2O-dependent shifts of −4 and −9 cm^{-1} for the modes at 1340 and 1575 cm^{-1}, respectively, were observed previously for the methylamine adduct of BSAO (*19*) and are ascribed to exchange of the C-3 hydrogen of the TPQ cofactor.

The rate of inactivation of N404A with methylamine was followed spectrophotometrically at various pHs. Methylamine concentrations equal to 10 times the K_m (determined from steady-state kinetics) were used. The initial rate of formation of the 380 nm peak was found to be a pH-independent value of 0.067 min^{-1}; however, the amount of inactivated species which accumulated in the steady state was pH-dependent (Figure 3).

The rate of reactivation for the inactive product Schiff base complex as a function of pH was also measured spectro-

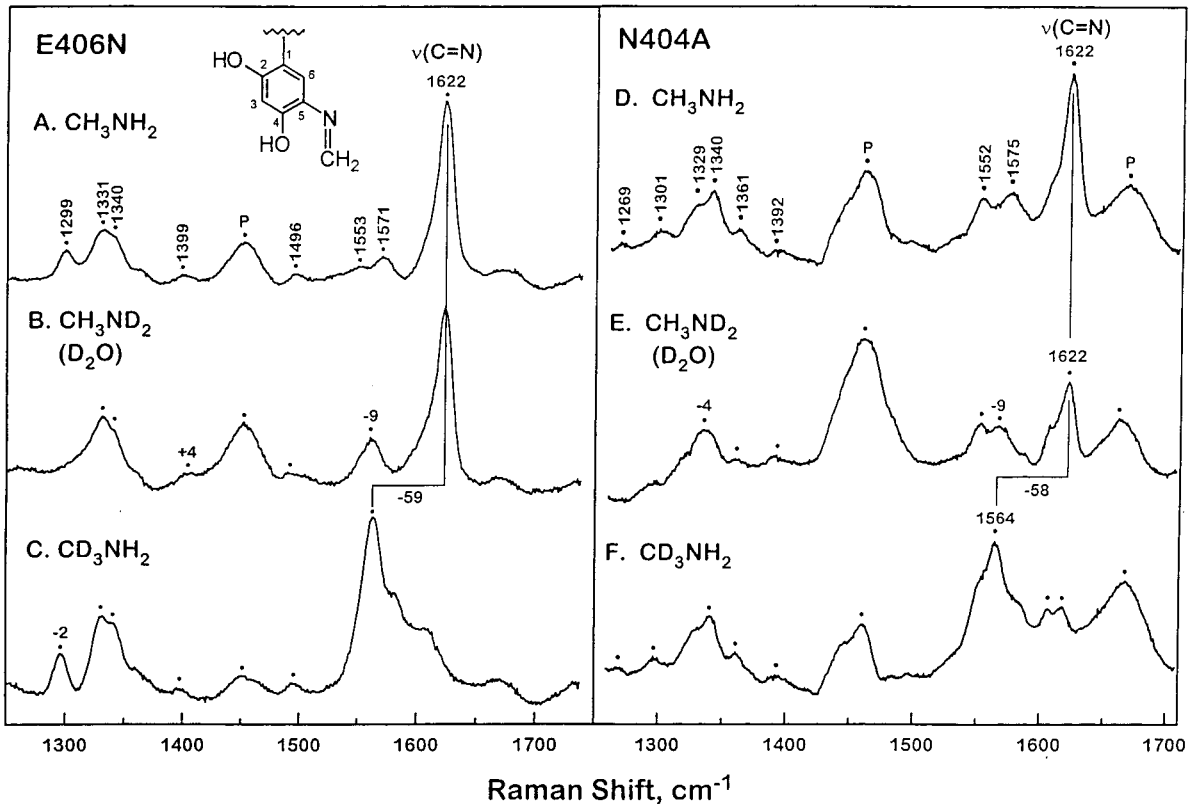

FIGURE 2: Raman spectra of methylamine adducts. Samples of E406N were prepared with (A) CH_3NH_2 in H_2O, (B) CH_3NH_2 in D_2O, and (C) CD_3NH_2 in H_2O (data from ref *16*). Samples of N404A (0.42 mM in TPQ) were prepared with (D) CH_3NH_2 in H_2O, (E) CH_3NH_2 in D_2O, and (F) CD_3NH_2 in H_2O. P indicates residual peaks from the apoprotein. Frequency shifts relative to spectrum A are indicated above peaks, and peaks with frequencies identical to those of spectrum A are unlabeled.

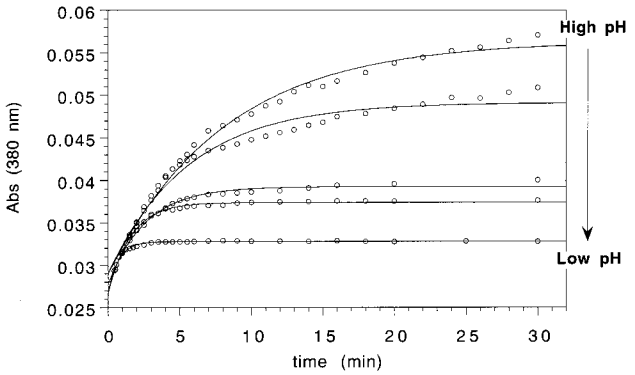

FIGURE 3: Formation of the inactive PSB complex at various pHs. Methylamine at a concentration equal to $10K_m$ was added to N404A at pH 8.8, 7.9, 7.4, 6.9, and 6.5, and the reactions were followed spectrophotometrically at 380 nm. The data for each pH were fit to an equation for a single-exponential process.

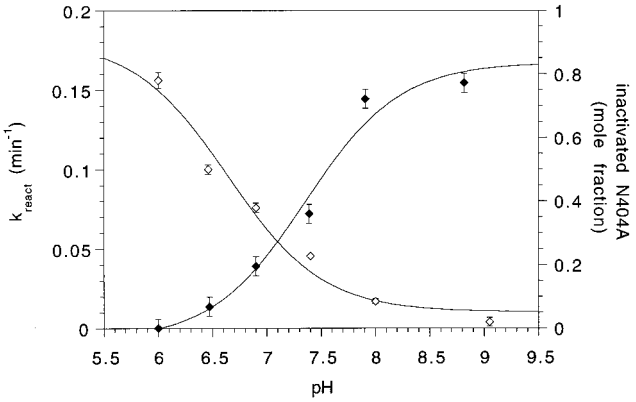

FIGURE 4: pH dependencies on the rate of reactivation of (◇) and steady-state accumulation of (♦) the PSB complex with methylamine.

photometrically. After incubation of a sample of N404A at pH 9 with methylamine for 1.5 h, excess substrate was removed concomitant with exchange into a buffer with a lower IS (10 mM KPP_i, pH 9.0). The sample was then diluted into a buffer at the desired pH and a much greater IS (300 mM) and the reaction followed spectrophotometrically to measure the rate of reactivation. The rate was found to vary with pH, displaying a dependency which was the reciprocal of that of the steady-state accumulation of the inactivated species (Figure 4).

Steady-State Parameters of N404A. $(k_{cat}/K_m)_{Am}$. k_{cat}/K_m for N404A with respect to amine as the substrate was determined over a range of pHs with methylamine (Figure 5A) and for several amines at pH 7.4 (Table 1). Results with the WT enzyme indicate the same pH dependence on k_{cat}/K_m for methylamine as N404A (*16*); however, the rate with N404A is decreased 1000-fold relative to that with WT.

k_{cat}. The pH profile for k_{cat} is displayed in Figure 5B. There is no observable pH dependence on k_{cat} for N404A over the pH range in which activity was assayed. These results are in marked contrast to the pH dependence of k_{cat} for WT HPAO, which displays a bell-shaped curve with rates slower than that of N404A below pH 6.3 and faster rates above this pH (*16*).

$(k_{cat}/K_m)_{O_2}$. k_{cat}/K_m with respect to oxygen was determined with N404A at various pHs (data not shown), and the values exhibited a dependence similar to that of the WT enzyme, except for a 50-fold decrease in maximal activity (*20*).

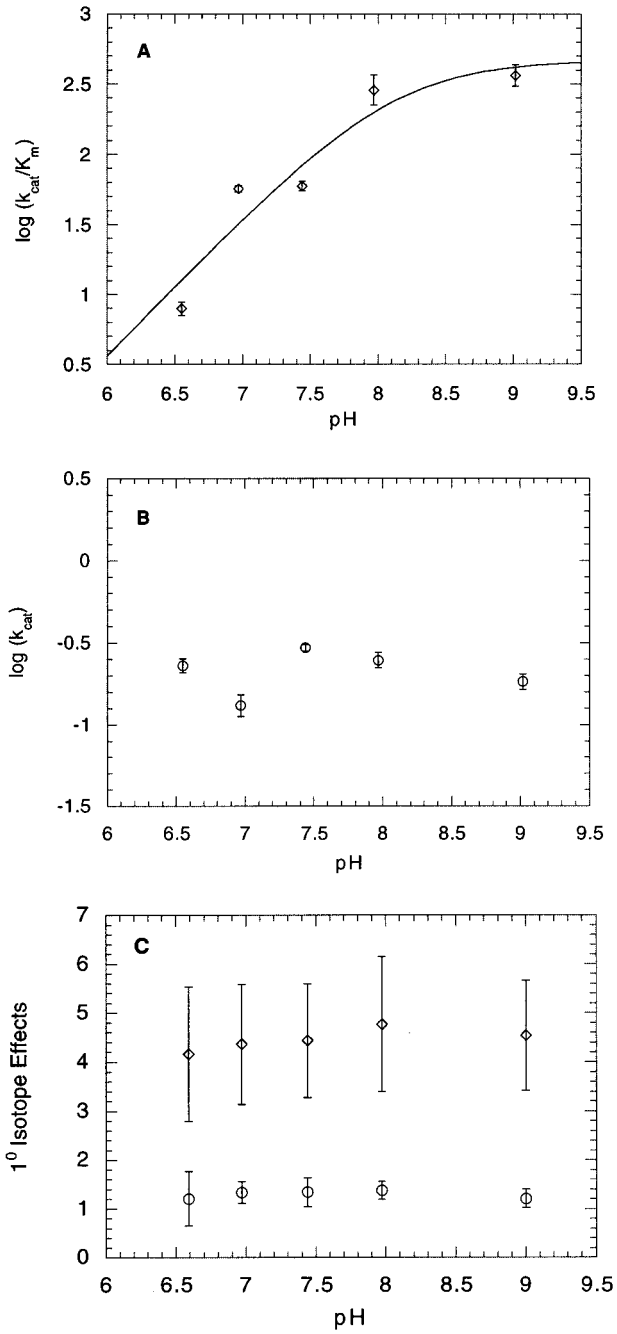

FIGURE 5: pH profile for N404A activity with methylamine. (A) Plot of log(k_{cat}/K_m) vs pH. The curve fit is for a single pK_a. (B) Plot of log(k_{cat}) vs pH. (C) Plot of primary isotope effects for k_{cat}/K_m (◇) and k_{cat} (○) vs pH.

Steady-State UV−Vis Experiments. The steady-state accumulation of an intermediate along the catalytic pathway was probed spectrophotometrically. When the intermediate was incubated with saturating levels of methylamine, two changes in the spectrum of N404A were readily apparent: bleaching of the oxidized cofactor at 492 nm and the concomitant formation of a peak at ca. 310 nm (data not shown), both occurring on a time scale consistent with catalysis (the 380 nm peak forms more slowly). The 310 nm peak is attributed to the reduced cofactor (aminoquinol) formed after hydrolysis of the product Schiff base, based on comparison to model compounds and anaerobic substrate-reduced enzyme (*21*, *22*).

Table 1: Kinetic Summary of WT HPAO and N404A[a]

	WT		N404A	
substrate	k_{cat} (s^{-1})	k_{cat}/K_m (M^{-1} s^{-1})	k_{cat} (s^{-1})	k_{cat}/K_m (M^{-1} s^{-1})
MeAm	3.19 ± 0.05[b]	$(6.4 \pm 0.5) \times 10^4$[b]	0.296 ± 0.013	59 ± 4
EtAm	3.94 ± 0.07	$(4.9 \pm 0.4) \times 10^4$	0.493 ± 0.018	110 ± 8
PhEtAm	3.18 ± 0.30	$(1.3 \pm 0.3) \times 10^5$	0.442 ± 0.006	300 ± 10
O_2	2.92 ± 0.05[c]	$(2.1 \pm 0.1) \times 10^5$[c]	0.318 ± 0.015	$(4.2 \pm 0.6) \times 10^3$

[a] Assays conducted with respect to amine as the substrate were performed at pH 7.44, at IS = 300 mM, and at ambient O_2 concentrations (258 μM at 25 °C) which were shown to be saturating. The assay with respect to O_2 as the substrate was conducted at pH 7.44, at IS = 300 mM, and at a methylamine concentration of $10K_m$ (50 mM). [b] From ref *16*. [c] From ref *20*.

$^{D}k_{cat}/K_{m-MeAm}$ and $^{D}k_{cat}$. The deuterium kinetic isotope effects on k_{cat}/K_m and k_{cat} were determined using CH_3NH_2 and CD_3NH_2 as substrates. A pH-independent value of approximately 4 was observed (Figure 5C) for k_{cat}/K_m, similar to the isotope effect found with the WT enzyme (*16*). The primary KIE on k_{cat} is close to unity (Figure 5C) and is also pH-independent. The insensitivity of $^{D}k_{cat}$ to pH is analogous to that found with WT HPAO (*16*).

Temperature Rescue of TOPA Biogenesis. N404A purified from yeast showed little redox stain, indicative of a lack of active cofactor. Digestion patterns from limited proteolysis with V8 protease were similar to those of the WT protein (data not shown), indicating that the protein was not misfolded (*16*). In addition, analysis by ICP atomic emission spectroscopy indicated that the levels of copper were similar to that found in the WT enzyme. Attempts to rescue cofactor biogenesis with the addition of formamide were unsuccessful, but heating the cofactor-depleted protein at 37 °C showed a dramatic increase in redox stain after 24 h. This result was quantified by reaction of the protein with phenylhydrazine before and after heating; without heating, N404A typically contained 5−10% cofactor, whereas after 24 h, yields ranged from 40 to 60%.

To quantify the temperature dependence of cofactor biogenesis in N404A, samples were incubated at various temperatures and aliquots removed as a function of time for titration with phenylhydrazine. Due to the much higher molar adsorptivity of the phenylhydrazone adduct versus that of the underivatized cofactor (35 600 vs 1600 M^{-1}, as determined by [^{14}C]phenylhydrazine radioactive labeling for this mutant; for the experimental method, see ref *15*), an accurate measure of cofactor percentage was easily achieved using this method. The rate of biogenesis was determined at 30, 37, and 45 °C, and the results are shown in Table 2. Higher temperatures could not be used as nonlinearity of data ensued, presumably due to nonspecific protein denaturation competing with cofactor formation. When ln(k) was plotted versus $1/T$, the slope indicated an enthalpy of activation of 9 kcal/mol. This value is significantly larger than the value of 3 kcal/mol for WT HPAO (*23*).

Qualitative Studies of Cofactor Biogenesis. N404A expressed in *H. polymorpha* was heated at 37 °C, and the reaction was followed spectrophotometrically to determine if the slow rate of biogenesis would allow observation of intermediates normally short-lived in the process for the WT protein. Only peaks corresponding to species also found during WT biogenesis (*23*) were observed.

Relationship between Cofactor Content and Catalytic Activity. Three samples from a single preparation of N404A were aliquoted and either maintained at 4 °C or heated for 18 h at 30 or 37 °C, respectively. Following quantitation of TPQ in each sample by phenylhydrazine titration, equal amounts of enzyme (based on cofactor concentration) were added to a standard enzyme assay (pH 7.44, MeAm = $5K_m$). The rates from the three single reactions were 0.212, 0.230, and 0.232 s^{-1}, respectively, indicating that the catalytic rate is proportional to the concentration of TPQ.

Table 2: Temperature Dependence of TPQ Biogenesis in N404A[a]

k (h^{-1})	T (°C)
0.0042	30
0.0165	37
0.0833	45

[a] Determined in 50 mM KP_i at pH 7.1.

DISCUSSION

Inactivation of N404A with Methylamine. From the crystal structure of several amine oxidases, a highly conserved asparagine residue (404 in the *H. polymorpha* enzyme) is found to be situated close to the face of the redox cofactor, TPQ or TOPA quinone (*10*−*13*), suggesting an important role for this residue in positioning of the cofactor, during either biogenesis, catalysis, or both. Previous work on another highly conserved amino acid, E406, showed that when this residue was mutated to an asparagine residue, the TPQ ring became more mobile, resulting in the rapid accumulation of an inactive enzyme species during turnover with methylamine (*17*). The species was identified as a deprotonated PSB of TPQ, on the basis of its characterization by UV−vis and resonance Raman spectroscopies. Thus, determining if a similar intermediate would be observed when N404 was mutated to alanine was of interest to us, due to the expected cavity created in the active site by this change.

The accumulation of a similar inactive species was observed when N404A was incubated with methylamine, as shown in Figures 1 and 2. In Figure 1, the time course is shown for formation of the PSB, represented by the 380 nm peak, at pH 9. While the 480 nm peak corresponding to oxidized TPQ disappears relatively rapidly (the reaction is essentially complete at 1 min), the 380 nm peak grows in slowly over the course of 1 h. This is consistent with results from steady-state kinetics where rapid inactivation of enzyme was not observed. This is in contrast to those for E406N, where rapid accumulation of the 380 nm peak was observed concomitant with obervable enzyme inactivation.

To identify positively the 380 nm species formed when N404A was mixed with methylamine, resonance Raman

spectroscopy was utilized (Figure 2, right). The N404A adduct behaved like E406N in the appearance of a C═N stretch at 1622 cm^{-1} that shifted with CD_3NH_2 but not in deuterated solvent. The failure to observe any shift in the C═N peak in D_2O indicates that the imine nitrogen is not protonated.

The PSB complex is only formed with methylamine, and not with the larger substrates ethylamine and phenethylamine, similar to the results found with E406N. Since the chemical reactivities are expected to be similar among these amines (cf. Table 1), the inhibitory differences observed among the three substrates are likely due to the differing steric constraints on the abilities of the respective product Schiff bases to adopt nonproductive orientations.

The effect of pH on inactivation was studied over the pH range of 6.5−9.0; no effect was observed on the initial rate, but the steady-state amount of intermediate which acccumulated was pH-dependent (Figure 3). The pH-independent rate of inactivation (0.067 min^{-1}) is different from that found with E406N, where a pK_a of around 7 was found to gate the process. This pK_a was assigned to a histidine residue normally found hydrogen-bonded to E406; it was postulated that disruption of the Glu−His interaction lowers the pK_a of the histidine, allowing it to be deprotonated and the mutant to form an inactive complex with methylamine during turnover. N404A forms the same inactivated species, but with a different pH dependence, supporting the previous arguments made for E406N.

Although pH does not affect the rate of inactivation, it was found to influence the amount of inactive species which accumulated under steady-state conditions. This suggests that while inactivation is pH-independent, reactivation is dependent, such that as the pH is decreased the rates of reactivation and inactivation become comparable. The rate of reactivation was measured directly and found to be pH-dependent in a manner which was the reciprocal of the steady-state accumulation of the 380 nm species (Figure 4). A pK_a of approximately 6.8 controls the reactivation process, and is tentatively assigned to the nitrogen of the product Schiff base complex. The pK_a is similar to that found for other highly delocalized Schiff bases (*24*), and it is expected that the hydrolysis reaction would proceed much faster with the nitrogen protonated (*25*). The pH-independent rate of inactivation indicates that the pK_a of the product Schiff base is shifted out of the range of 6.5−9 on the enzyme in the active conformation. This is not surprising as the enzyme is expected to keep the nitrogen protonated during turnover near physiologic pHs, likely through electrostatic interactions with the active site base Asp319; this residue is proximal to the nitrogen of the Schiff base as revealed by its position relative to the terminal hydrazine N-1 in the crystal structure of a 2-hydrazinopyridine−enzyme adduct (*26*).

Interpretation of Steady-State Kinetics. The pH profile of k_{cat}/K_m for the mutant enzyme with methylamine is shown in Figure 5A. Although the pH dependency is similar to that of the WT protein, the maximal value is reduced a dramatic 1000-fold with N404A. The data for the WT enzyme indicate that there are two pK_as which contribute to the profile, one at 8.1 and one at 9.9 (*16*). The lower pK_a is similar to that found in the pH profile for N404A, and has been assigned in WT to the ionization of the active site base (D319). Among all of the HPAO proteins studied to date (WT and mutants), only an active site base mutant has been observed to have a different pK_a (*15*, *16*); on the basis of these lines of evidence, the lower pK_a of 8.1 has been assigned to the active site base. Due to the similarity between the pH profiles for WT and N404A, it is reasonable to assign pK_as in a similar manner for both proteins.

The 10^3-fold reduction in k_{cat}/K_m for N404A was further explored by measurement of the primary KIE on k_{cat}/K_m; a pH-independent value of approximately 4 was observed (Figure 5C), analogous to the value found with the WT enzyme (*16*). This value is less than the KIE of 11.5 found previously with an amine oxidase from bovine serum; the reduced KIE in the yeast enzyme may reflect only partial rate limitation by C−H abstraction from the substrate Schiff base in the reductive half-reaction or a less symmetrical reaction barrier for C−H bond cleavage (*27*).

The similar KIEs and pH dependencies found with mutant and WT enzymes indicate a mechanism in which most of the oxidized enzyme is in a nonproductive orientation prior to substrate binding (Scheme 1), with the small fraction of enzyme in the correct conformation proceeding in a manner identical to that of the WT protein. On the basis of the 1000-fold reduction in k_{cat}/K_m found with N404A and all substrate amines studied (Table 1), only 0.1% of the mutant enzyme is expected to be in a catalytically productive conformation. The tendency of free enzyme to adopt a nonproductive orientation is likely caused by the increased mobility of the cofactor, as evidenced by its ability to form the nonproductive PSB complex during turnover. With E406N, the nonproductive orientation was suggested to be one with TPQ "flipped", with the reactive C-5 carbonyl oxygen pointing away from the active site base.

A flipped, and somewhat mobile orientation for TPQ in the resting state of N404A is also indicated by recent resonance Raman studies, which measured the exchange rate of the C-3 TPQ hydrogen in D_2O and the C-5 carbonyl oxygen in $H_2{}^{18}O$ (*28*). For WT HPAO, where the TPQ ring is shown to be fixed in the active orientation in the crystal structure, the C-5 carbonyl oxygen exchanges rapidly, whereas no exchange of the C-3 proton is detected. With D319E and D319N, mutants where the TPQ ring is believed to be fixed in a flipped orientation in the free, oxidized enzyme, the rates of C-3 exchange are relatively rapid, whereas rates of C-5 exchange are slow (*15*, *28*).

In contrast to these patterns, exchanges at both the C-5 and C-3 positions are rapid with N404A (i.e., fully exchanging in 1 h, the dead time for sample preparation in these experiments). This suggests a dynamically flipping TPQ, together with efficient addition of $H_2{}^{18}O$ to the C-5 carbonyl of cofactor once TPQ accesses the productive orientation. A similar conclusion is implied anecdotally by phenylhydrazine titrations; all of the TPQ in N404A can react with the labeling reagent, but it does so at a rate much diminished from that of the WT enzyme (about 1 h vs a few minutes, respectively, with an excess of phenylhydrazine). These results corroborate and supplement the picture of the mutant's active site generated from the steady-state kinetic data; the cofactor in the free, oxidized form of N404A exists mainly in a catalytically nonproductive orientation (a thermodynamic consideration, which affects k_{cat}/K_m and presumably reaction with phenylhydrazine), with sufficient mobility to allow dynamic equilibration between accessible conformers (a

Scheme 1

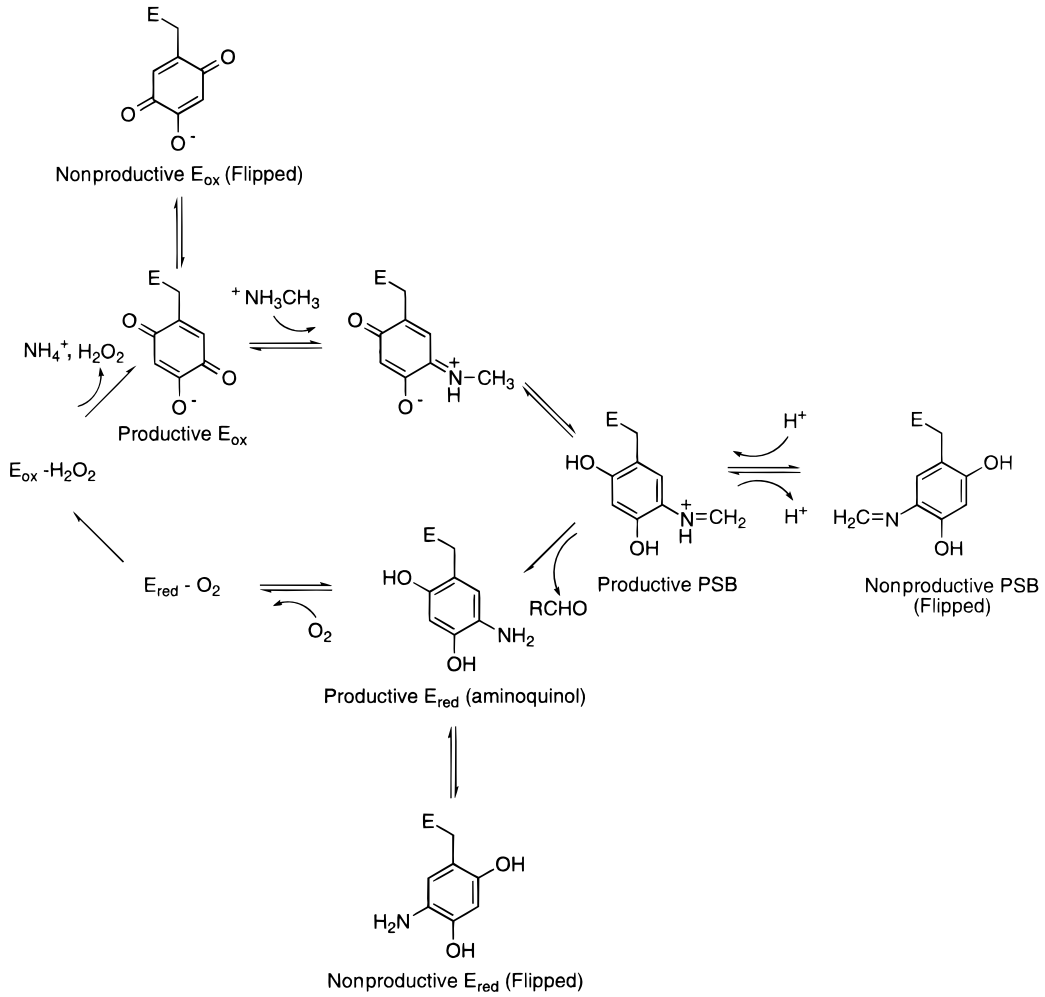

kinetic consideration, which affects the ability of cofactor to exchange at both the C-5 and C-3 positions).

The inability of the flipped TPQ in N404A to turn over productively is in contrast to findings with D319E, where the cofactor was concluded to be in a nonproductive orientation in the resting state, but was induced to flip upon binding substrate (*15*). In the case of D319E, both the pH dependence and KIE for k_{cat}/K_m differed from WT, in contrast to the results with N404A. This difference highlights the importance of the relative conformation of the TPQ ring to the activity of the CAOs, in contrast to recent work which suggested that ring flipping of the cofactor would be mechanistically unimportant (*12*). To clarify the nomenclature currently used in the literature, we suggest the terms productive and nonproductive (Scheme 1) to refer to the two distinct TPQ orientations which can occur when TPQ is not liganded to copper. Both the productive and nonproductive conformations have previously been called TPQ-OFF (*12*).

The pH profile for k_{cat}/K_m for the oxidative half-reaction was also measured and compared to WT data. As with the pH profile for methylamine, there appears to be no difference in the pH dependencies for the reactions catalyzed by WT and mutant enzymes, although the maximal rate is reduced 50-fold (Table 1). These results imply a similar phenomenon to that of the resting, oxidized cofactor; the reduced cofactor without oxygen bound exists mainly (95%) in a nonproducitve conformation, with the small fraction of the enzyme in the productive orientation reacting in a manner similar to that of the WT protein. Without the amide group of N404 to orient TPQ in a productive mode, it appears that both oxidized and reduced forms of the cofactor in free enzyme can easily adopt alternate conformational modes which preclude turnover.

The pH-independent profile of k_{cat} for N404A is different from that of WT HPAO, and is likely the result of a change in the rate-determining step during turnover. Whereas pK_as of 7.9 and 8.8 are found in the WT profile (*16*), no pK_as appear to titrate for the mutant enzyme in the pH range of 6.5−9 (Figure 5B). Steady-state incubation of N404A and methylamine indicates that some form of reduced enzyme accumulates during turnover, similar to that of WT enzyme. It is possible that a slow, pH-independent conformational change of this species is responsible for the observed activity profile with N404A. The nonproductive orientations found for both the resting, oxidized enzyme and methylamine-reduced enzyme increase the likelihood of this possibility. It should be noted that aldehyde release is not likely to be rate-limiting since methylamine, ethylamine, and phenethylamine all displayed similar values of k_{cat}; formaldehyde, acetaldehyde, and phenacetaldehyde would be expected to be released with differing off rates.

Biogenesis Studies. N404A obtained after standard isolation protocols for HPAO contained very little cofactor, indicated qualitatively by the comparatively faint stain

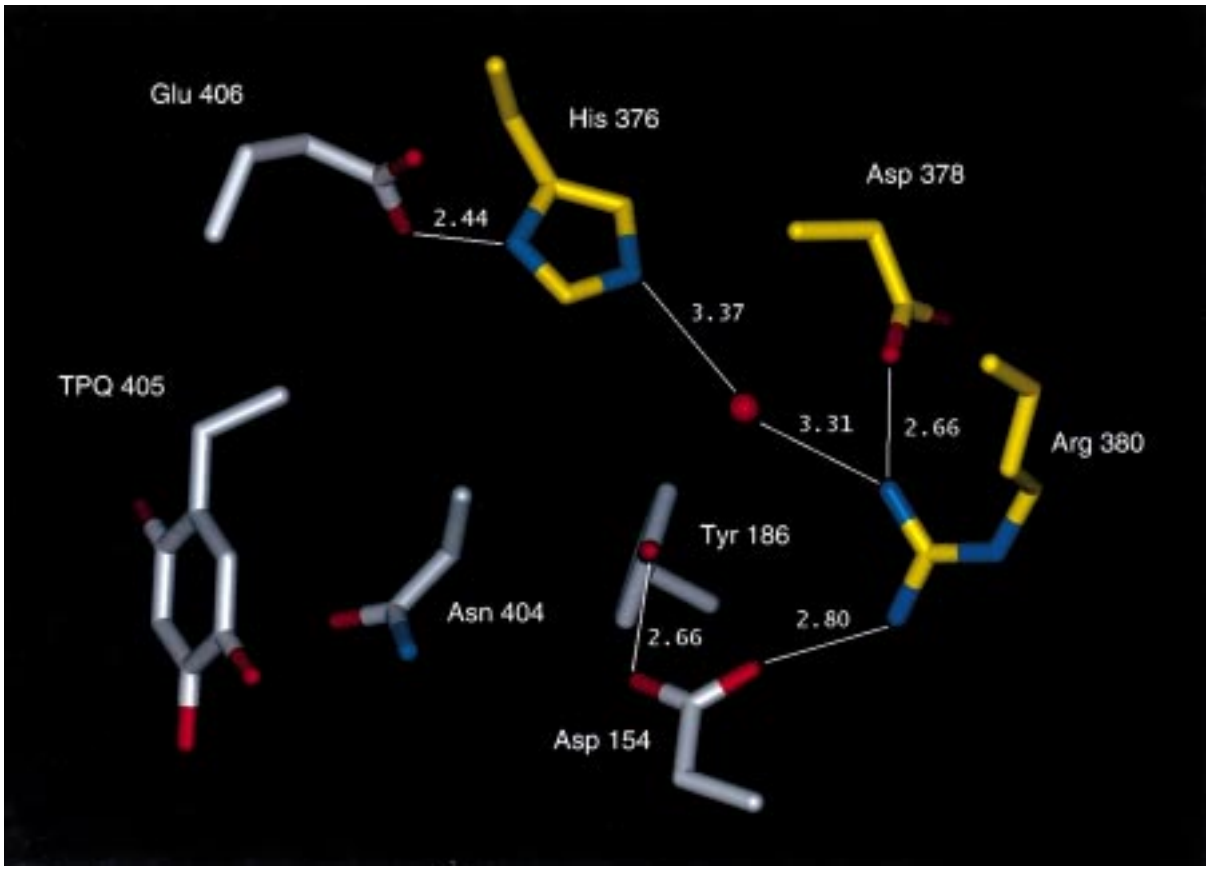

FIGURE 6: Proposed loop structure for HPAO. Residues from the A subunit are gray and those from the B subunit yellow. Oxygen atoms are red, and nitrogen atoms are blue. Connectivity is shown by solid lines between residues, and hydrogen bonding distances are given for these interactions (from PDB file 1A2V).

observed by redox cycling assay and quantitatively by phenylhydrazine titration and 480 nm absorbance. However, when isolated protein was heated at 37 °C, a dramatic increase in the amount of active cofactor was observed. To quantitate the observed temperature dependence of biogenesis, samples were incubated at 30, 37, and 45 °C and aliquots were removed occasionaly for quantitation by reaction with phenylhydrazine. The calculated rates of biogenesis are shown in Table 2. A plot of ln(k) versus 1/T for these three rates yielded an approximate value of 9 kcal/mol for the enthalpy of activation, as compared with 3 kcal/mol obtained for the WT enzyme (*23*).

Biogenesis of a low-cofactor sample was followed spectrophotometrically at 37 °C, but no UV−vis species were observed that differed significantly from those detected in WT biogenesis. Since the mechanism for biogenesis is less well characterized than that for catalysis, it is difficult to interpret the meaning of the large temperature dependence found with N404A; however, in light of the results found with catalysis, it is a distinct possibility that the large enthalpy of activation is related to the impared ability of the mutant to properly position either the precursor tyrosine or biogenetic intermediates that occur in the production of TPQ in N404A.

Nature of the Interaction between N404 and TOPA. The amide side chain of N404 resides proximal to the aromatic face of the TPQ ring in the crystal structure of WT HPAO, and a hydrogen bond between the amide nitrogen and π face of the cofactor appears likely (*13*). This type of amino/aromatic hydrogen bond is well documented in crystal structures and can contribute a significant amount of energy (*29*). This interaction may be further strengthened in the enzyme by means of an unusual hydrogen bond found between the N404 amide side chain oxygen and its own backbone amide nitrogen, which should make the side chain amide nitrogen less electronegative, thus increasing its hydrogen-donating ability.

Role of Consensus Site Residues. The sequence Asn-Tyr*-Asp/Glu-Tyr/Asn (residues 404−407 in the *H. polymorpha* enzyme) is highly conserved in all amine oxidases, with the Tyr* residue corresponding to the TPQ cofactor in the mature protein. Roles for these residues have been suggested (*30*), but a precise role has yet to be determined. It is interesting that N404 and E406 appear to have similar effects on positioning of the TPQ ring, as evidenced by the accumulation of the inactive PSB complex during turnover of both mutants with methylamine, despite the lack of a clear through-space interaction between the two residues.

Close examination of the crystal structures of the enzymes from *H. polymorpha*, *Escherichia coli*, and pea seedling shows that a hithertofore unidentified loop may exist between the Asn and Glu/Asp residues, conserved in spatial arrangement though variable in composition (Figure 6). Residues corresponding to Asn404 of the A subunit in HPAO and His376 and Asp378 of the B subunit are conserved among all three structures, whereas the position occupied by Glu406 is an aspartate in the *E. coli* and pea seedling enzymes. Tyr186 in HPAO (A subunit) is also a tyrosine in the pea seedling enzyme, but is replaced by a tryptophan in the *E. coli* structure. In all three cases, however, the π faces of the aromatic residues define the same spatial plane and

appear to buttress the position of the Asn residue. The other elements shown in Figure 6 which stabilize the loop structure in HPAO are different in the other enzyme structures.

The existence of this loop provides a reasonable framework for understanding the connectivity between N404 and E406 and their roles in maintaining the integrity of the active site structure. In particular, there are two distinct features to consider: the relative rates of catalysis to inactivation by formation of the nonproductive PSB complex (i.e., k_{cat}/k_{inact}) and the general tendency to accumulate nonproductive, flipped intermediates during the catalytic cycle (i.e., k_{inact}/k_{react}).

In the case of N404A, it is expected that with the amide functionality removed a cavity is opened near the cofactor, allowing flipping of the PSB to occur. However, interaction between the planar methylene of the PSB and remaining β-methyl carbon of the alanine residue appears to exert a moderate influence on positioning of the TPQ cofactor, resulting in a relatively slow rate of inactivation (high value for k_{cat}/k_{inact} of $\approx$265). In the case of E406N, it is expected that an only slightly altered arrangement of the active site is maintained at low pHs, where His376 remains protonated and able to hydrogen bond to the amide carbonyl oxygen of the mutated Asn406 side chain. As with N404A, the result is the observation of a slow rate of inactivation of the PSB, as evidenced by a large value for k_{cat}/k_{inact} ($\approx$200). However, as the pH is increased, His376 becomes deprotonated and the active site residues rearrange to accommodate a new hydrogen-bonding network in the loop. The specifics of this reorganization are not known, but may reasonably be envisioned to include N404 in some manner, such that the positioning of TPQ is compromised. The small value for k_{cat}/k_{inact} ($\approx$25) found at high pHs with E406N indicates that the alteration to the active site structure under these conditions is more severe with respect to the PSB complex than the changes envisioned for N404A.

In contrast to k_{cat}/k_{inact}, which is a kinetic comparison, k_{inact}/k_{react} is a thermodynamic measure of the stability of a particular flipped conformation relative to its normal, catalytically competent one. In this regard, it is interesting that several enzyme forms in the reaction catalyzed by N404A have large values for this parameter; the values can be deduced for the free, oxidized (1000:1) and free, reduced enzyme (20:1) from the corresponding reductions in k_{cat}/K_m, and calculated directly for the PSB (17.2:1, pH 9) from the measured rates of k_{inact} and k_{react}. This trend implies that the mature cofactor in HPAO has the ability to thermodynamically access an energetically more favorable conformation, but is prevented from doing so by kinetic restraint of flipping motions by key active site residues, including N404, E406, and other highly conserved residues (*16*, *17*). Indeed, circumstantial evidence suggests that this is the case with all CAOs; the crystal structures of different WT CAOs are found to contain the TPQ ring in both the catalytically productive and nonproductive orientations (*10*−*13*).

The ability of CAOs to thermodynamically access catalytically nonproductive orientations would seem to be counterproductive for normal enzyme activity, and in this respect, it is surprising that the active site architecture has been constructed in such a manner. However, the active site of CAOs is unique in that it must carry out the dual functions of biogenesis and catalysis. It is believed that multiple conformational states arise during biogenesis (*12*), whereas only one active conformation is expected during catalysis; thus, the active site in this class of enzymes represents a carefully balanced compromise between these conflicting requirements. N404 has been shown herein to be an essential element in striking this balance, as its mutation to alanine results in the cofactor readily displaying biogenesis-like characteristics of cofactor motion during catalysis.

One aspect of these results which is not currently understood is the differing ratios of k_{inact}/k_{react} found with the various forms of N404A. It is possible that crystal structures of either N404 or E406 mutants with methylamine may help elucidate the specific interactions between the protein and substrate which influence this phenomenon; these structures are currently being pursued.

Implications for Intersubunit Communication. The proposed pathway of communication between E406 and N404 runs between the subunits of the dimeric protein, along the unique "embracing arms" of the structure. It is interesting that one end of the arm contains TPQ and the rest of the consensus site sequence, while the other end contains residues which interact with the active site on the other subunit. It has been posited previously that the embracing arms may be sites for intersubunit communication (*10*, *11*), and the specific pathway proposed herein may provide a molecular basis for this proposal. The existence of such an intersubunit communication could result in half-site reactivites for either biogenesis or catalysis. Half-site reactivity during catalysis is currently an unresolved point for the TOPA-containing enzymes studied thus far; there are results that support and do not support such a phenomenon (*26*, *31*, *32*). Future work will utilize site-directed mutagenesis to elucidate the role of the other residues involved in the conserved loop and their potential influence on communication between the two subunits of the enzyme.

ACKNOWLEDGMENT

We thank Stephen A. Mills for his help with ICP. We also thank Joanne Dove and Dr. Julie Plastino for their intellectual contributions to this work.

REFERENCES

1. Klinman, J. P. (1996) *Chem. Rev. 96*, 2541−2561.
2. Yu, P. H., and Zuo, D. M. (1997) *Diabetologia 40*, 1243−1250.
3. Boomsma, F., van Veldhuisen, D. J., de Kam, P. J., in't Veld, A. J. M., Mosterd, A., Lie, K. I., and Schalekamp, M. A. D. H. (1997) *Cardiovasc. Res. 33*, 387−391.
4. Janes, S. M., Mu, D., Wemmer, D., Smith, A. J., Kaur, S., Maltby, D., Burlingame, A. L., and Klinman, J. P. (1990) *Science 248*, 981−987.
5. Anthony, C. (1996) *Biochem. J. 320*, 697−711.
6. Holt, A., Alton, G., Scaman, C. H., Loppnow, G. R., Szpacenko, A., Svendsen, I., and Palcic, M. M. (1998) *Biochemistry 37*, 4946−4957.
7. Matsuzaki, R., Fukui, T., Sato, H., Ozaki, Y., and Tanizawa, K. (1994) *FEBS Lett. 351*, 360−364.
8. Cai, D., and Klinman, J. P. (1994) *Biochemistry 33*, 7647−7653.
9. Janes, S. M., Palcic, M. M., Scaman, C. H., Smith, A. J., Brown, D. E., Dooley, D. M., Mure, M., and Klinman, J. P. (1992) *Biochemistry 31*, 12147−12154.
10. Parsons, M. R., Convery, M. A., Wilmot, C. M., Yadav, K.

D. S., Blakeley, V., Corner, A. S., Phillips, S. E. V., McPheron, M. J., and Knowles, P. F. (1995) *Structure 3*, 1171−1184.
11. Kumar, V., Dooley, D. M., Freeman, H. C., Guss, J. M., Harvey, I., McGuirl, M. A., Wilce, M. C. J., and Zubak, V. (1996) *Structure 4*, 943−955.
12. Wilce, M. C. J., Dooley, D. M., Freeman, H. C., Guss, J. M., Matsunami, H., McIntire, W. S., Ruggiero, C. E., Tanizawa, K., and Yamaguchi, H. (1997) *Biochemistry 36*, 16116−16133.
13. Li, R., Klinman, J. P., and Matthews, F. S. (1998) *Structure 6*, 293−307.
14. Dunn, B., and Wobbe, R. C. (1996) in *Current Protocols in Molecular Biology* (Ausubel, F. M., Brent, R., Kingston, R. E., Moore, D. D., Seidman, J. G., Smith, J. A., and Struhl, K., Eds.) Vol. 2, pp 13.0.1−13.13.9, Wiley, New York.
15. Plastino, J. J., Green, E. L., Sanders-Loehr, J., and Klinman, J. P. (1998) *Biochemistry* (submitted for publication).
16. Hevel, J. M., Mills, S. A., and Klinman, J. P. (1998) *Biochemistry* (submitted for publication).
17. Cai, D., Dove, J., Nakamura, N., Sanders-Loehr, J., and Klinman, J. P. (1997) *Biochemistry 36*, 11472−11478.
18. Loehr, T. M., and Sanders-Loehr, J. (1993) *Methods Enzymol. 226*, 431−470.
19. Nakamura, N., Moenne-Loccoz, P., Tanizawa, K., Mure, M., Suzuki, S., Kilnman, J. P., and Sanders-Loehr, J. (1997) *Biochemistry 36*, 11479−11486.
20. Su, Q., and Klinman, J. P. (unpublished results).
21. Mure, M., and Klinman, J. P. (1993) *J. Am. Chem. Soc. 115*, 7117−7127.
22. Hartmann, C., Brzovic, P., and Klinman, J. P. (1993) *Biochemistry 32*, 2234−2241.
23. Williams, N. K., and Klinman, J. P. (1998) (manuscript in preparation).
24. Sakmar, T. P., Franke, R. R., and Khorana, H. G. (1991) *Proc. Natl. Acad. Sci. U.S.A. 88*, 3079−3083.
25. Bruylants, A., and Feytmants-De Medicis, E. (1970) in *Chemistry of the Carbon-Nitrogen Double Bond* (Patai, S., Ed.) pp 473−492, Interscience, New York.
26. Wilmot, C. M., Muresonance Ramanay, J. M., Alton, G., Parsons, M. R., Convery, M. A., Blakeley, V., Corner, A. S., Palcic, M. M., Knowles, P. F., McPherson, M. J., and Phillips, S. E. V. (1997) *Biochemistry 36*, 1608−1620.
27. Grant, K. L., and Klinman, J. P. (1989) *Biochemistry 28*, 6597−6605.
28. Green, E. L., Nakamura, N., Klinman, J. P., Dooley, D. M., Tanizawa, K., and Sanders-Loehr, J. (1998) (manuscript in preparation).
29. Mitchell, J. B. O., Nandi, C. L., McDonald, I. K., Thorton, J. M., and Price, S. L. (1994) *J. Mol. Biol. 239*, 315−321.
30. Choi, Y.-H., Matsuzaki, R., Suzuki, S., and Tanizawa, K. (1996) *J. Biol. Chem. 37*, 22598−22603.
31. DeBiase, D., Agostinelli, E., DeMatteis, G., Mondovi, B., and Morpurgo, L. (1996) *Eur. J. Biochem. 237*, 93−97.
32. Janes, S. M., and Klinman, J. P. (1991) *Biochemistry 30*, 4599−4605.

BI981541S